

ACOUSTICAL LETTER

Basic study of practical prediction of sound insulation performance of double window

Yohei Tsukamoto[1,2,*], Kaoru Tamai[2], Kimihiro Sakagami[2], Takeshi Okuzono[2] and Yoshihiro Tomikawa[1]

[1]*YKK AP Inc., YKK AP R&D Center, 1 Ogyu, Kurobe, Toyama, 938–8612 Japan*
[2]*Environmental Acoustics Laboratory, Department of Architecture, Graduate School of Engineering, Kobe University, Rokko, Nada-ku, Kobe, 657–8501 Japan*

(*Received 4 April 2022, Accepted for publication 13 May 2022*)

Keywords: Double window, Prediction, Sound insulation

1. Introduction

The sound insulation performance of windows is an important feature of a building's acoustic environment. Double windows are an extremely effective solution for practical sound insulation on windows. A double window is a window structure comprising two frames and two glass window panes (Fig. 1). The sound insulation performance of windows is usually evaluated by the sound reduction index: *SRI*. The sound transmission of double partitions has been examined theoretically. Simple and practical methods of predicting *SRI* have been proposed [1,2]. Although the sound insulation performance of double windows has been examined in some studies [3,4], few experiments to assess actual windows have been reported. For windows, some special differences such as gaps of window frames are expected to affect the *SRI*. Some method for predicting the *SRI* of a double window is necessary to design a room's acoustic environment.

This study was conducted to propose a practical method for predicting the *SRI* of a double window. We first used some equations based on existing sound transmission theories through double constructions for application to double windows. The calculated values were compared with measured *SRI*s of double windows. Based on numerous measured values, correction of the prediction equation was attempted. As described herein, the windows were assumed to be sliding windows.

2. Application of existing transmission theories of double constructions

2.1. Existing theories

Figure 2 presents a model of a double partition structure. The following symbols are defined in this paper as indicated in Fig. 2. Therein m_1 and m_2 respectively denote the surface densities of partitions (window panes) 1 and 2, kg/m^2. R_1 and R_2 respectively represent the *SRI*s of the partitions 1 and 2, dB. The variable ρ represents the air density, kg/m^3, c stands for the sound velocity in air, m/s, and d denotes the cavity depth, m.

For most double constructions, *SRI* can be expressed simply as shown below [1].

$$SRI \cong 10\log[\{(K_1+K_2)\cos kd - 2K_1K_2\sin kd\}^2 + \eta_0^2] \tag{1}$$

Therein, k signifies the wavenumber ($=\omega/c$), ω stands for the angular frequency, and η_0 is the loss factor of the partitions. Values K_1 and K_2 respectively denote the normalized impedance of partitions. Assuming that the partition impedance depends on the partition surface density, the two equivalent partition impedances are expressed using the measured *SRI* of each partition R_1 and R_2, as shown below.

$$K_1 = 10^{\frac{R_1}{20}}, \quad K_2 = 10^{\frac{R_2}{20}} \tag{2}$$

The sound transmission of double-leaf constructions is well known to have a significant peak because of the mass–air–mass resonance at low frequencies. The resonance frequency f_0 is approximated as follows.

$$f_0 = \frac{1}{2\pi}\sqrt{\frac{\rho c^2}{d}\left(\frac{1}{m_1}+\frac{1}{m_2}\right)} \tag{3}$$

In addition, at frequencies higher than $kd = 1$, the *SRI* has many dips because of the standing waves normal to the two partitions in the cavity. The lower frequency limit at which the standing waves occur, f_d, is given below.

$$f_d = \frac{c}{2\pi d} \tag{4}$$

With the frequencies shown by Eqs. (3) and (4), Rindel organized the *SRI* of double constructions into three frequency ranges and approximated the equations for each frequency as presented below [1].

$$SRI \cong \begin{cases} 20\log(K_1+K_2) & (f < f_0) \\ R_1+R_2+20\log\left(\dfrac{f}{f_d}\right)+6 & (f_0 < f \le f_d) \\ R_1+R_2+6 & (f_d < f) \end{cases} \tag{5}$$

If the measured *SRI* at random incidence of each partition is substituted in R_1, R_2, K_1, and K_2 with Eq. (2), then the *SRI* of the double constructions is derived. In the case of a double window, the measured values of each window R_1 and R_2 are regarded as including the effect of the characteristics of each window such as the gaps of the window frames.

Another theory of the sound transmission of double constructions is also referred. The theory by Brekke considers

*e-mail: y_tukamoto@ykkap.co.jp
[doi:10.1250/ast.43.335]

Fig. 1 Illustration of a double window.

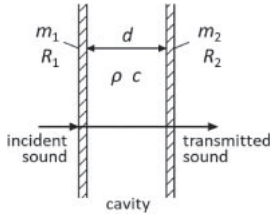

Fig. 2 Model of sound transmission through a double partition (window).

the effect of the absorption of the inside surface of the perimeter in the cavity. The equation is [2]

$$SRI \cong R_1 + R_2 + 10\lg\left(\alpha \cdot \frac{d \cdot U}{S}\right) \tag{6}$$

where α is the absorption coefficient of the inside surface of the cavity perimeter, U stands for the partition perimeter length, m, and S signifies the partition area, m^2. If the cavity has no absorbent material, then the equivalent absorption coefficient α is given as shown below [2].

$$\alpha \cong \begin{cases} 0.5 & (d \leq 20\,\text{mm}) \\ 0.01/d & (d > 20\,\text{mm}) \end{cases} \tag{7}$$

Figure 3 presents a comparison of the calculated result of these two theories and measured result of a benchmark double window. Table 1 shows data of the benchmark window. Measured results of the respective windows (outer and inner windows) are shown in the same graph. Measurements were taken in accordance with JIS A 1416:2000 [5], which is

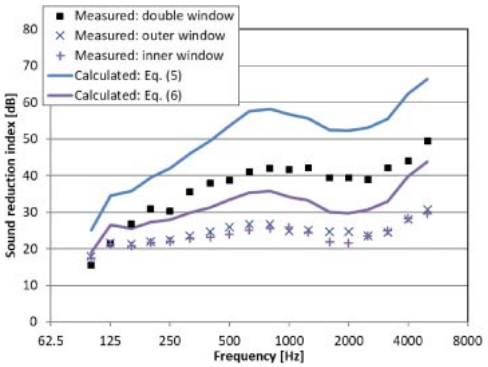

Fig. 3 Sound reduction indices of double windows. Calculated values by Eqs. (5) and (6) and measured values of the benchmark double window and each single window are shown.

Table 1 Data of benchmark double window.

Window type	sliding window
Glass type (outside)	single, 5 mm thickness
Glass type (inside)	single, 5 mm thickness
Cavity depth	84 mm
Window width	1720 mm
Window height	1800 mm

equivalent to ISO 10140-2 [6]. Figure 3 shows that the *SRI* of a double window is much greater than that of either window alone. However, the *SRI* of a double window is less than that of a single window at around 100 Hz because of the mass–air–mass resonance. In this case, f_0 of the double window is calculated as 83 Hz by Eq. (3). These major tendencies of the sound transmission characteristics agree with the general trend of double-leaf constructions [1].

As for existing theories, the value calculated using Eq. (5) is more than 10 dB greater than the measured value over all frequencies. The value calculated using Eq. (6) is less than the measured value at frequencies higher than 315 Hz by more than 5 dB. The prediction by Eq. (6) reportedly agrees with the *SRI* of double constructions above the cut-off frequency ($= c/2d$), at which the half-wavelength coincides with the cavity depth [3]. In this case, the frequency is calculated to 2046 Hz. However, it did not match in the case of this double window. Even when the measured values of windows were substituted into R_1 and R_2, these calculated values disagree with the measured values obtained for the double window. Therefore, these predictive theories for double constructions cannot be applied to predict the *SRI* of a double window in their original forms. Although the value of Eq. (5) disagrees in quantitative terms with the measured value, the trend in frequency characteristics apparently corresponds qualitatively. This finding suggests that more accurate prediction might be possible with appropriate correction.

2.2. Parameter effects

In this section, the cavity depth effect is examined. The *SRI*s of the double windows were measured under three conditions: cavity depths of 84 mm, 114 mm, and 144 mm. Additionally, calculations using Eqs. (5) and (6) were conducted under the same cavity depth conditions as in the measurement. The measured and calculated results are presented respectively in Fig. 4 and Fig. 5.

According to Fig. 4, the cavity depth effect appears below middle frequencies. When the cavity of a double window is deeper, the *SRI* at low frequencies is larger. The cavity depth has no effect above approximately 1000 Hz. According to results shown in Fig. 5, the cavity depth does not affect the calculation by Eq. (6). The calculation results by Eq. (5) are mutually similar at high frequencies, irrespective of the cavity depth. However, at low frequencies, the deeper cavity condition shows larger *SRI*. The trend of the cavity depth effect calculated using Eq. (5) qualitatively resembles that of the experimentally obtained result.

2.3. Combination of theories

A prediction method of *SRI* of a double window is developed based on Eq. (5), which shows a similar trend to that of the measured value of the double window. We consider

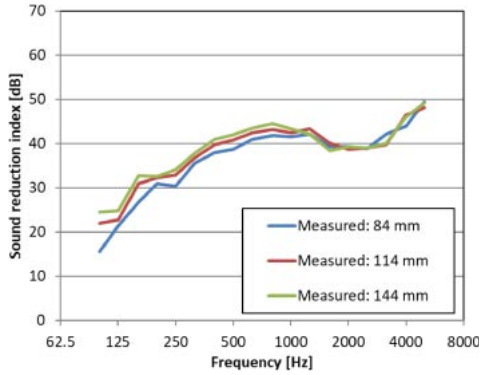

Fig. 4 Measured sound reduction indices of double windows with cavity depths of 84, 114, and 144 mm.

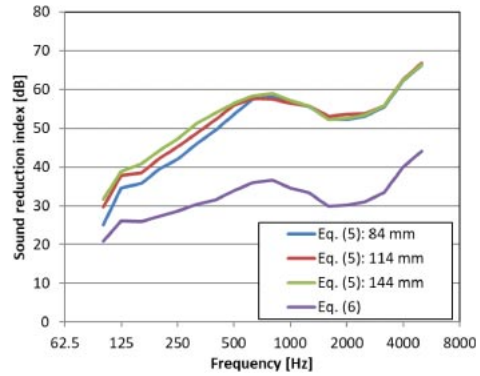

Fig. 5 Calculated sound reduction indices of double constructions theories, Eqs. (5) and (6), with cavity depths of 84, 114, and 144 mm.

introduction of a correction term in Eq. (5). Brekke derived an equivalent absorption coefficient, Eq. (7), for double constructions without absorbent materials, based on experimentally obtained results [2]. Similarly, the equivalent absorption coefficient term in Eq. (6) is added to Eq. (5). Then, we propose a prediction method as

$$SRI \cong \begin{cases} 20\log(K_1+K_2)+10\log\left(\alpha\cdot\dfrac{d\cdot U}{S}\right) & (f<f_0) \\ R_1+R_2+20\log\left(\dfrac{f}{f_\mathrm{d}}\right)+6 & \\ \quad +10\log\left(\alpha\cdot\dfrac{d\cdot U}{S}\right) & (f_0<f\le f_\mathrm{d}) \\ R_1+R_2+6+10\log\left(\alpha\cdot\dfrac{d\cdot U}{S}\right) & (f_\mathrm{d}<f) \end{cases} \tag{8}$$

where the equivalent absorption coefficient α is expressed as Eq. (7). The value calculated using Eq. (8) is compared with the measured values for a benchmark double window (Table 1) in Fig. 6. Figure 6 shows that the value calculated using Eq. (8) seems to agree with the measured value. Especially at frequencies higher than 500 Hz, the differences between calculated and measured values are less than 4 dB. However, a still larger discrepancy exists at low frequencies. This trend, which was apparent for other test window

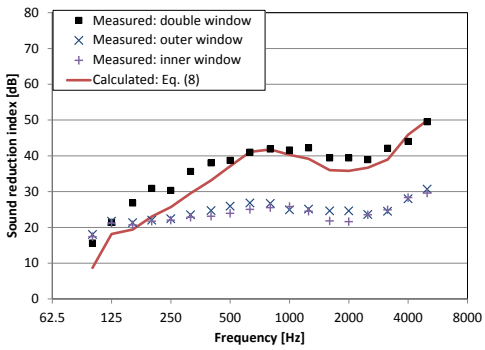

Fig. 6 Sound reduction indices of double window. Calculated value of Eq. (8) and measured values of the benchmark double window (Table 1) and each single window are shown.

specimens, remains as a difficulty hindering practical methods for predicting *SRI*.

3. Correction for double window

Correction for the equivalent absorption coefficient α is investigated based on Eq. (8). Another α for double windows is derived from multiple measured data of *SRI* of double windows.

First, multiple *SRI* data of double windows were collected. Then the trend was analyzed. For this study, 41 datasets of *SRI* of double windows were collected. All of these double windows were composed of two sliding windows with single-glass glazing. All measurements were conducted according to JIS A 1416 [5] in the same laboratory. The areas of these test windows were 2.32–4.84 m^2, with cavity depths of 84–146 mm, and glass thickness of 3 mm or 5 mm.

Differences between these measured results and the results calculated using Eq. (8) are averaged in each 1/3 octave band. Figure 7 shows the averaged differences ΔR. One trend is that ΔR has larger values at lower frequencies. The highest value of ΔR is about 8 dB at 200 Hz.

Based on the measured results, a linear regression equation of ΔR is derived as a function of the logarithm of frequency as follows.

$$\Delta R = -1.716\ln f + 14.168 \tag{9}$$

This linear regression of ΔR is also portrayed in Fig. 7. To calculate the equivalent absorption coefficient α for double windows, Eq. (9) is applied.

$$\alpha = \frac{1}{100d}\cdot 10^{\frac{\Delta R}{10}} \tag{10}$$

For reference, Fig. 8 presents a comparison of α by Eqs. (9) and (10) and α by Eq. (7) for 0.1 m cavity depth. The values of α found using Eqs. (9) and (10) show higher values at lower frequencies. It is more than 0.4 at 100 Hz; it is about 0.1 at high frequencies. However, α by Eq. (7) is constantly 0.1 for all frequencies. The application of α derived from Eqs. (9) and (10) affects the calculated *SRI* by Eq. (8) at low frequencies. Therefore, we attempted to correct the prediction of *SRI* by applying α for double windows derived from ΔR from Eqs. (9) and (10).

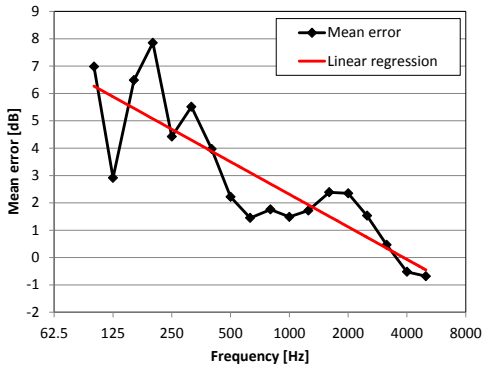

Fig. 7 Mean error between measured and predicted sound reduction indices of a double window with a single-glazed window. Red line shows linear regression of the mean error.

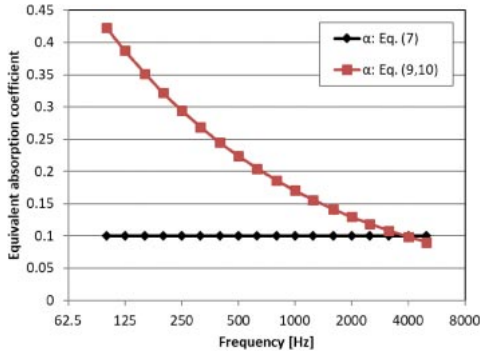

Fig. 8 Equivalent absorption coefficient from mean error between measured and predicted values ($d = 0.1$ m).

To verify this correction, the values calculated using Eqs. (8), (9), and (10) are compared with other *SRI* data for verification, which is not used to derive Eq. (9). Figure 9(A) shows three sets of data: measured values of a double window presented in Table 2, calculated values using Eq. (8) with α from Eqs. (9) and (10), and calculated values using Eq. (8) with α from Eq. (7). Figure 9(B) shows the absolute error between measured and respective calculated values. The absolute errors show significant improvement by α for double windows. The maximum absolute error decreased from about 8 dB to less than 4 dB. The mean absolute error (*MAE*) was 2.8 dB before correction and 1.1 dB after correction. Therefore, results indicate that introduction of a new equivalent absorption coefficient offers better prediction of the *SRI* of double windows.

4. Conclusion

A practical method for predicting the sound reduction index of double windows was studied based on existing theories for double-leaf constructions and experimentally obtained results. The combination of calculations by two sound transmission theories qualitatively agrees with the trend of the sound reduction index of double window. Additionally, the equivalent absorption coefficient for double windows was presented to improve prediction accuracy at low frequencies.

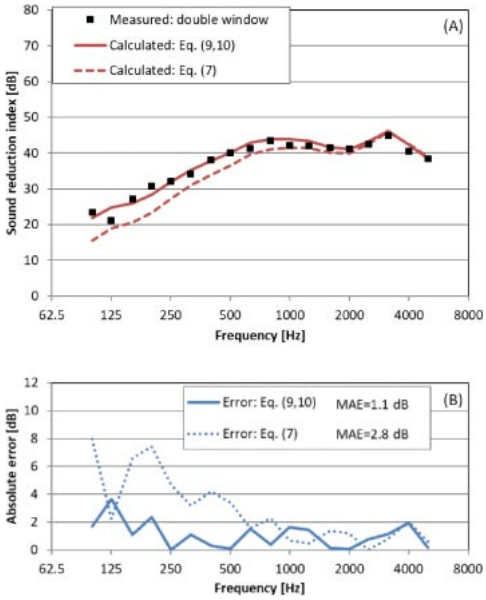

Fig. 9 (A) Sound reduction indices of double window calculated by Eqs. (8), (9) and (10), and calculated by Eqs. (7) and (8). (B) Absolute errors with measured values (before and after correction by the present method).

Table 2 Data of double window for verification.

Window type	sliding window
Glass type (outside)	single, 3 mm thickness
Glass type (inside)	single, 3 mm thickness
Cavity depth	186 mm
Window width	1650 mm
Window height	1300 mm

Although double windows with only single-glass glazing windows were considered in this paper, double windows with multiple glazing window are also widely used. In addition, a predicting method with predicted values of inner and outer windows should be more useful in practical work. The developments of these types of prediction methods are also important matters that will be the subject of future work.

References

[1] J. H. Rindel, *Sound Insulation in Buildings* (CRC Press, Boca Raton, 2018), Chap. 9.
[2] A. Brekke, "Calculation methods for the transmission loss of single, double and triple partitions," *Appl. Acoust.*, **14**, 225–240 (1981).
[3] J. D. Quirt, "Sound transmission through windows II. Double and triple glazing," *J. Acoust. Soc. Am.*, **74**, 534–542 (1983).
[4] A. J. B. Tadeu and D. M. R. Mateus, "Sound transmission through single, double and triple glazing. Experimental evaluation," *Appl. Acoust.*, **62**, 307–325 (2001).
[5] JIS A 1416:2000 Acoustics — Method for laboratory measurement of airborne sound insulation of building elements (2000).
[6] ISO 10140-2:2010 Acoustics — Laboratory measurement of sound insulation of building elements — Part 2: Measurement of airborne sound insulation (2010).